Supplementary Information for

AlphaFold2 has more to learn about protein energy landscapes

Devlina Chakravarty[1], Joseph W. Schafer[1], Ethan A. Chen[1], Joseph R. Thole[1,2], and Lauren L. Porter[1,2,*]

[1]National Center for Biotechnology Information, National Library of Medicine, National Institutes of Health, Bethesda, MD 20894
[2]Biochemistry and Biophysics Center, National Heart, Lung, and Blood Institute, National Institutes of Health, Bethesda, MD, 20892

*Correspondence: porterll@nih.gov

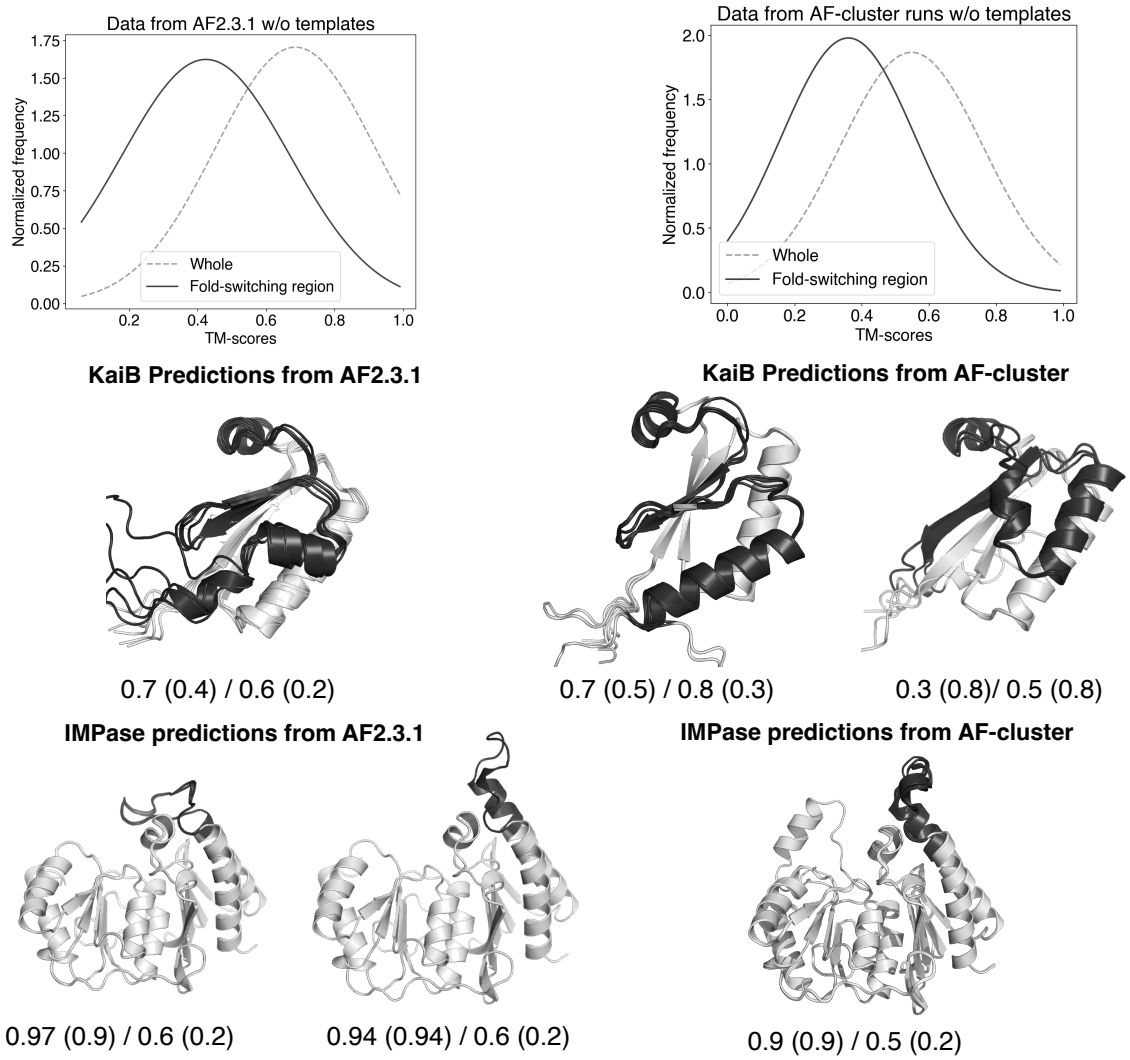

Figure S1. **TM-scores for fold-switching regions represent predictions of fold switchers more accurately than TM-scores of whole proteins**. Distributions of overall vs fold-switching region TM-scores for AF2.3.1 (upper left) and AF-cluster (upper right) demonstrate that whole-protein TM-scores overestimate prediction accuracies corresponding to regions of interest. Examples of predictions from AF2.3.1 and AF-clusters for KaiB and IMPase further demonstrate this point (fold-switching region is highlighted in black and the rest is grey). TM-scores relative to Fold 1 (left of /) and Fold 2 (right of /) are systematically higher for whole proteins (numbers without parentheses) compared to their fold-switching regions (in parentheses).

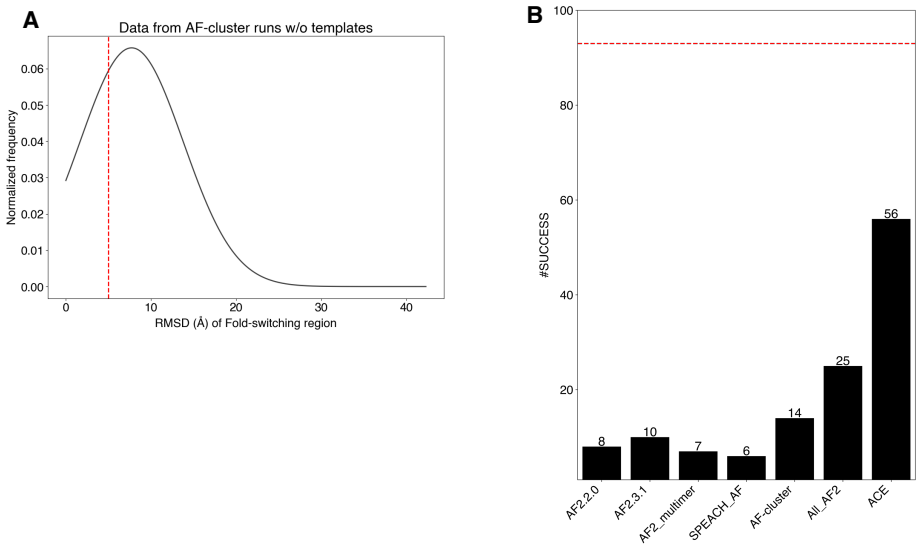

Figure S2. Assessing predictions by RMSD yields results similar to TM-score based assessments. Distribution of RMSD for the fold-switching region of AF-cluster predictions referenced against the fold-switching regions of the most similar experimentally determined structure is presented on the left panel (**A**), with threshold line at 5 Å. Prediction success measured by RMSD (**B**, fold-switching RMSD within 5 Å of experiment) yields results similar to TM-score (Figure 1 in main text).

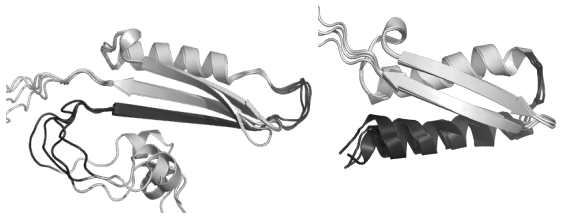

TM-scores (Whole/FS) - 0.6 (0.2) / 0.8 (0.4)

TM-scores (Whole/FS) - 0.5 (0.4) / 0.7 (0.4)

Figure S3. AlphaFold2 is likely overtrained on some structures. For example, Fold1 (PDBID: 2kxo) of MinE is predicted by inputting the full length MSA with templates into AF2.3.1, whereas Fold2 (PDBID:3r9j) is predicted by all models by inputting a single sequence (the sequence of MinE) with no templates. TM-scores relative to Whole/Fold-switching region (FS, black) are shown for full protein relative to experimentally determined structures (TM-scores relative to less similar fold in parentheses). Regions of the protein that don't switch folds are light gray.

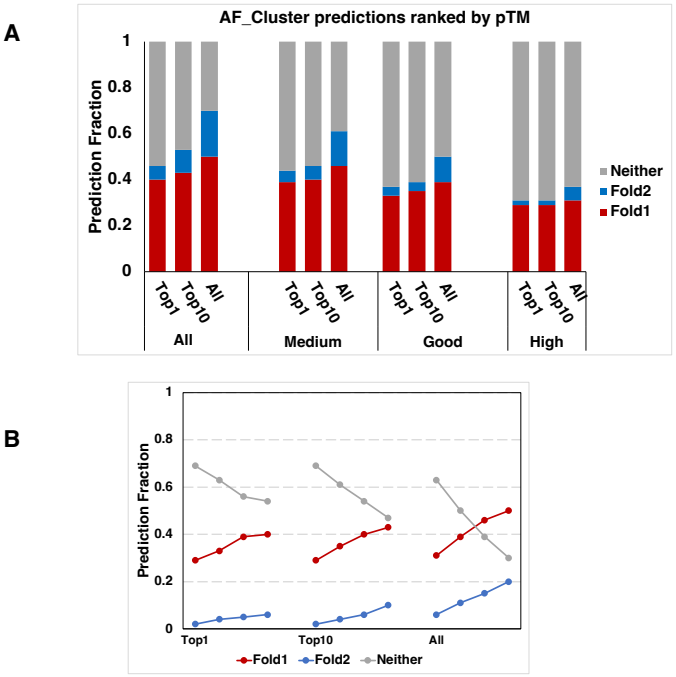

Figure S4. Ranking by predicted template modeling (pTM) score selects against experimentally observed conformations in favor of experimentally unobserved for AF-cluster predictions. (A) Bar-plot representation of the Prediction Fraction in Top1,Top10 and All ranked models. (B) Trendline plots showing the change in prediction success in categories –High (pTM>0.9), Good (pTM>0.7), Medium (pTM > 0.6), and All, respectively for Top1, Top10 and All predictions. Neither denotes predictions whose fold-switching regions had TM-scores < 0.6 relative to the experimentally determined structures of both Fold1 and Fold2.

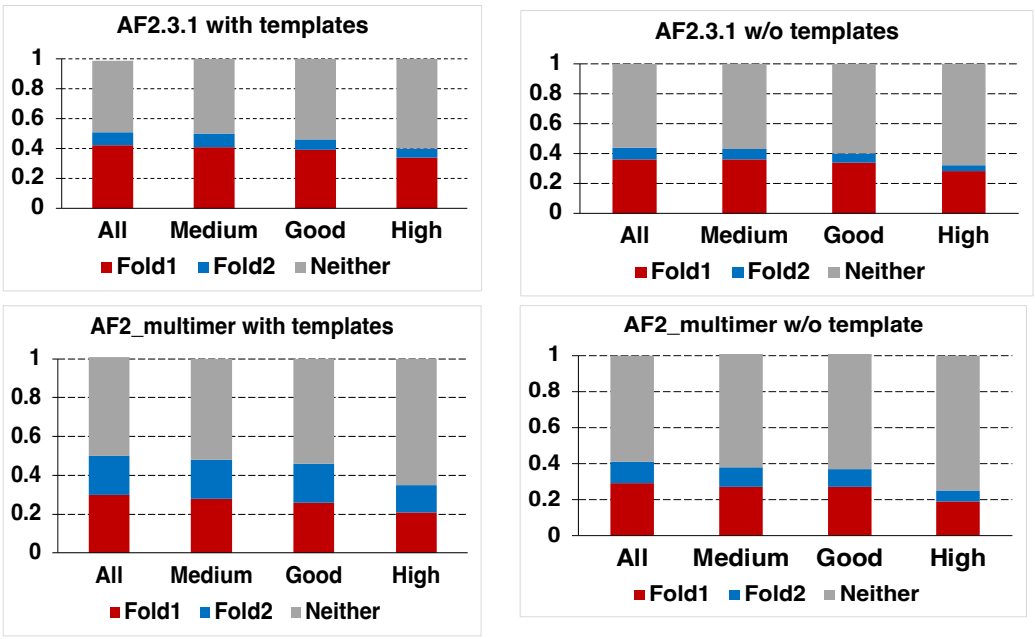

Figure S5. pLDDT scores select against experimentally determined conformations of fold-switching regions in all AF2.3.1. runs. Predictions are ranked by confidence (percentage of residues with pLDDT scores > 70). The categories are defined as - All, Medium (confidence > 70%), Good (confidence > 80%) and High (confidence >90%). Neither denotes predictions whose fold-switching regions had TM-scores < 0.6 relative to the experimentally determined structures of both Fold1 and Fold2.

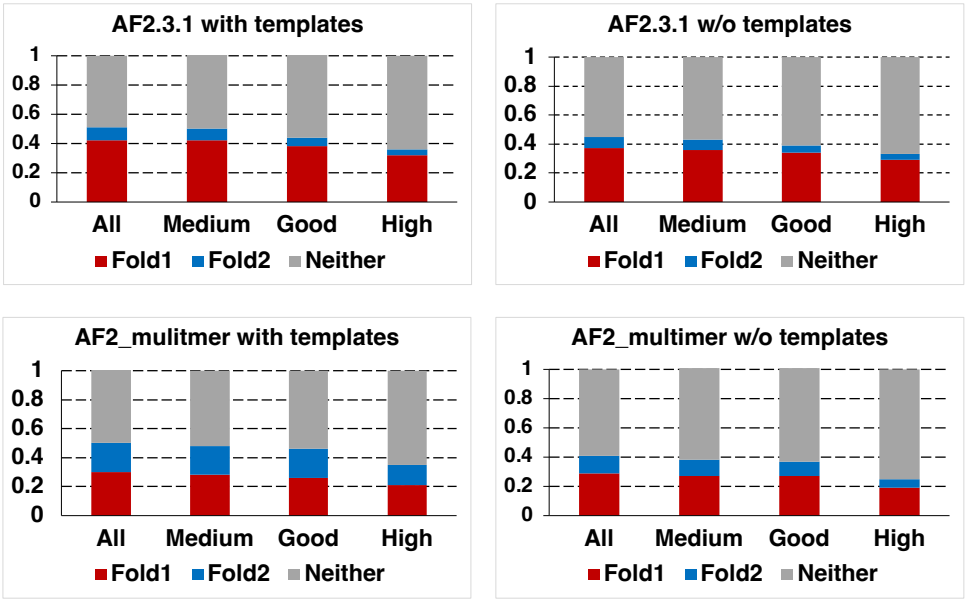

Figure S6. pTM scores select against experimentally determined conformations of fold-switching regions in all AF2.3.1. runs. Predictions are ranked by confidence (pTM score defined as - All, Medium (pTM ≥ 0.6), Good (pTM ≥ 0.7) and High (pTM ≥ 0.8). Neither denotes predictions whose fold-switching regions had TM-scores < 0.6 relative to the experimentally determined structures of both Fold1 and Fold2.

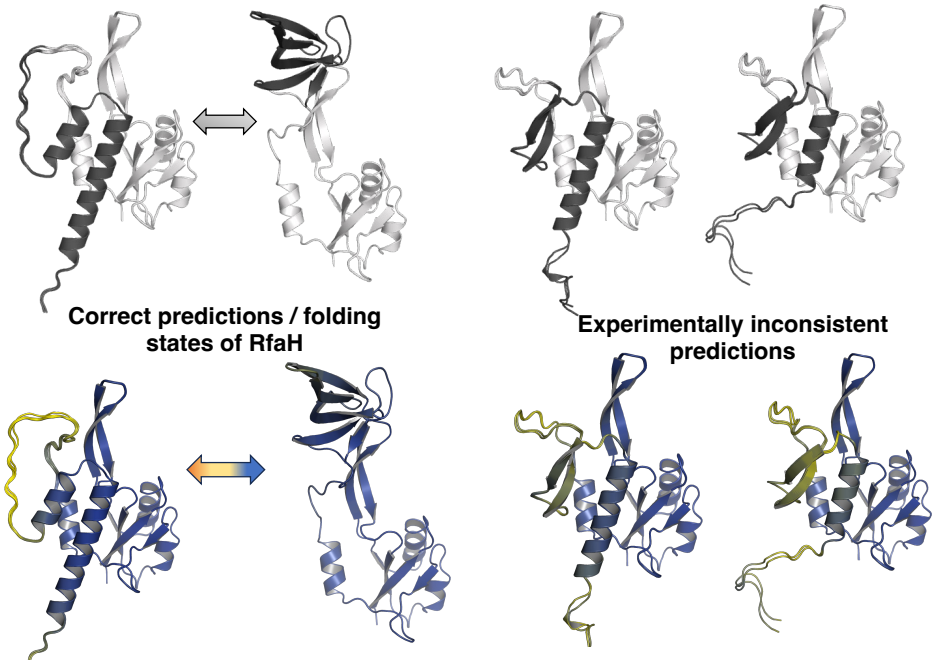

Figure S7. AF2 predicts experimentally inconsistent conformations of RfaH. Models corresponding to experimentally determined structures on left; experimentally inconsistent predictions shown on right. The figures below are colored by pLDDT scores, (color ranging from orange, yellow to blue, corresponding to pLDDT scores from 0 to 100). All predictions were generated from AF2_multimer (run without partner and no templates).

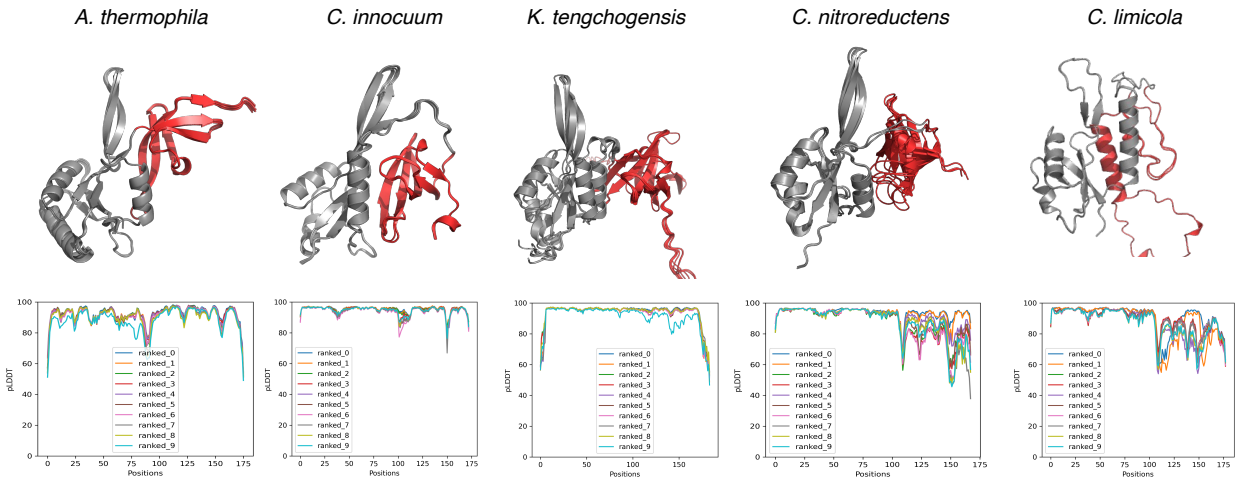

Figure S8. AlphaFold2.3.1 fails to predict the experimentally confirmed helical conformations in the C-terminal domains (CTDs) of 4/5 RfaH homologs. In all variants but *C. limicola*, only β-sheet CTDs (red) are predicted. Structurally conserved N-terminal domains are colored gray. pLDDT scores of all 10 models of each protein generated without templates are shown below their predicted structures. C-terminal domains comprise residues 115-end of protein.

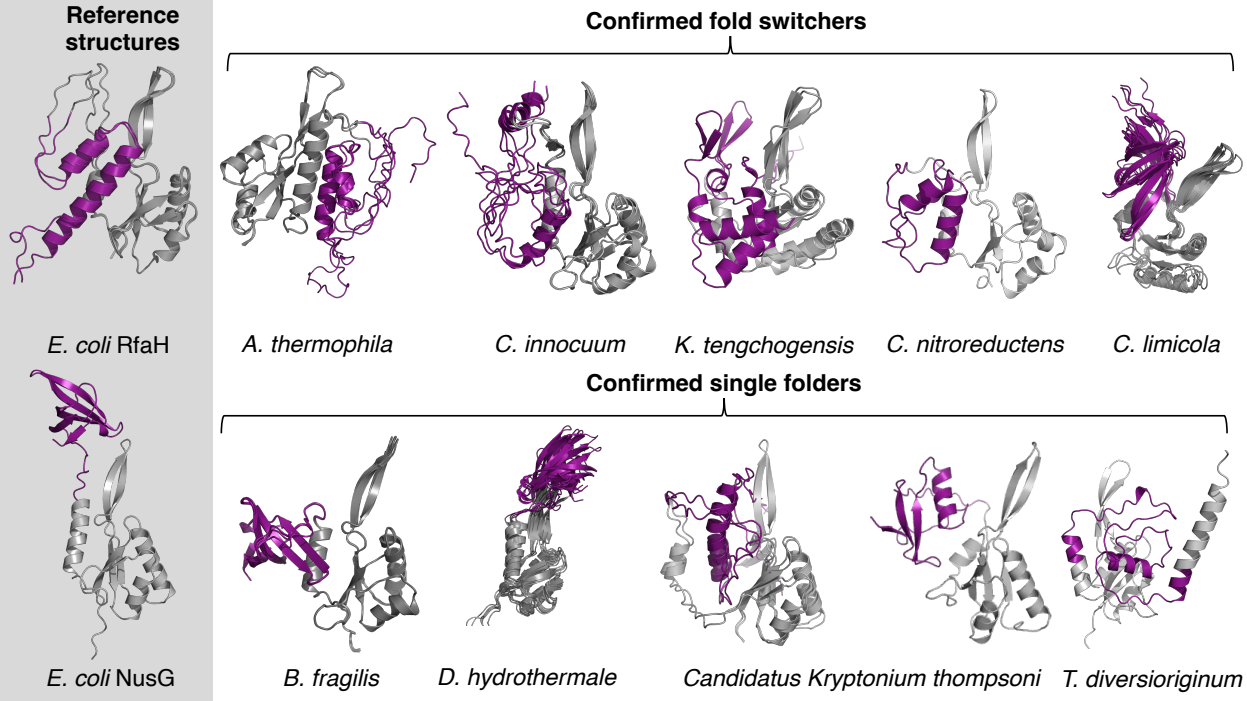

Figure S9. AF-cluster predictions cannot distinguish between RfaH homologs with helical C-terminal domains (CTDs, upper row) and β-sheet C-terminal domains (lower row). Further, pLDDT scores of all helical CTD predictions are low (average ≤50), further indicating that correct and incorrect predictions cannot be distinguished. All CTDs are colored purple; structurally conserved N-terminal domains are gray. Experimentally confirmed reference structures of *E. coli* RfaH and NusG are shown on the left column with the same color scheme.

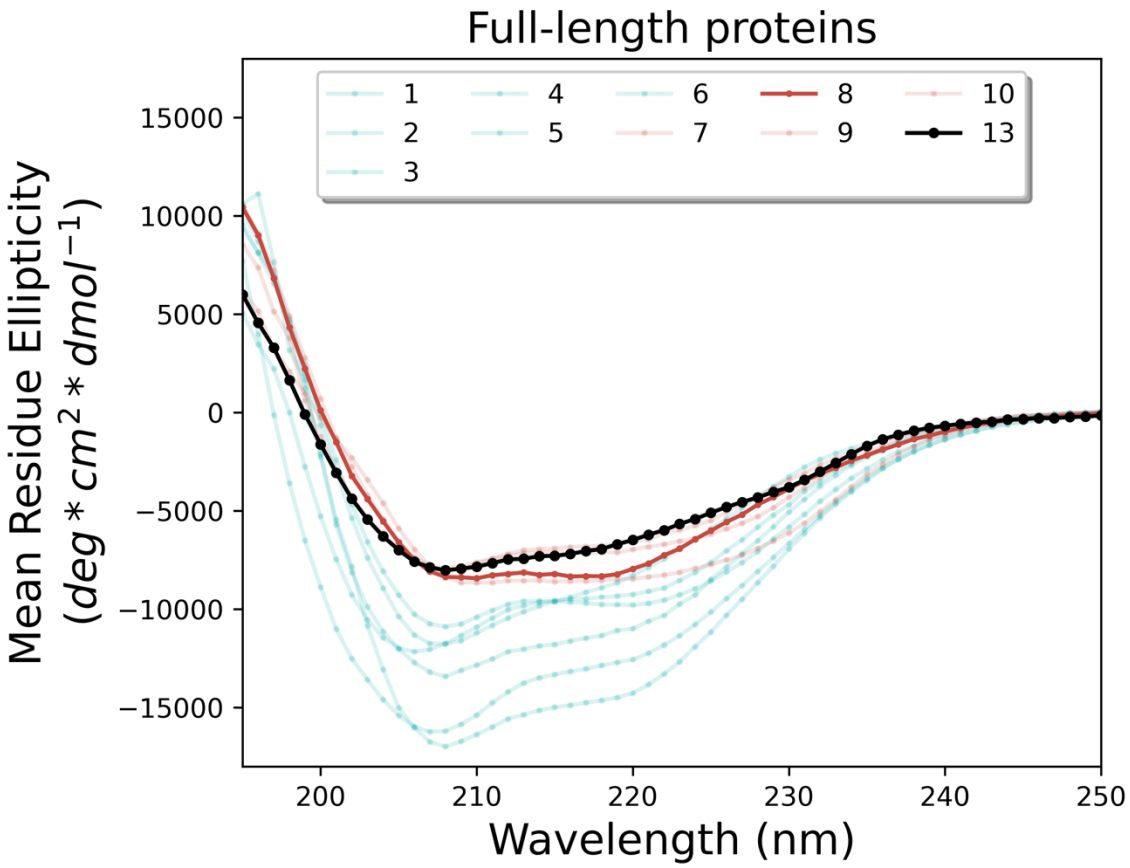

Figure S10. The circular dichroism spectrum of NusG Variant 13 (black) resembles single-folding NusGs with ground state β-sheet folds (red) rather than fold-switching NusGs with ground state α-helical folds (teal). CD spectra of all variants except for 13 were taken from reference 24 in the main text. AF-cluster predicted that it and Variant 8 (bold red) can assume helical folds, inconsistent with experimental evidence. The sequence of Variant 13 (Table S4) inserted into a pET-28a(+) vector was purchased through BioBasic, codon optimized for *E. coli*. Variant 13 was purified using Cytiva Hi-TRAP columns on an ÄKTA Pure at room temperature. Its 6x-His tag was cleaved overnight with biotinylated thrombin (Sigma Millipore) at 4°C while dialyzing in 100 mM potassium phosphate, 10% glycerol (v/v) pH 7.4 using a ThermoFisher dialysis cassette (10 kDa MWCO). The cleaved sample was again run on a Hi-TRAP column, and the unbound flow-through was then concentrated in a Millipore centrifugal concentrator (10 kDa MWCO) and subsequently polished through size exclusion chromatography with a Superdex 70 Increase 10/300 column (Cytiva) and was found to be monomeric. Its CD spectrum was collected on a Chirascan spectrometer (Advanced Photophysics) in 100 mM Phosphate, pH 7.6 at 9μM.

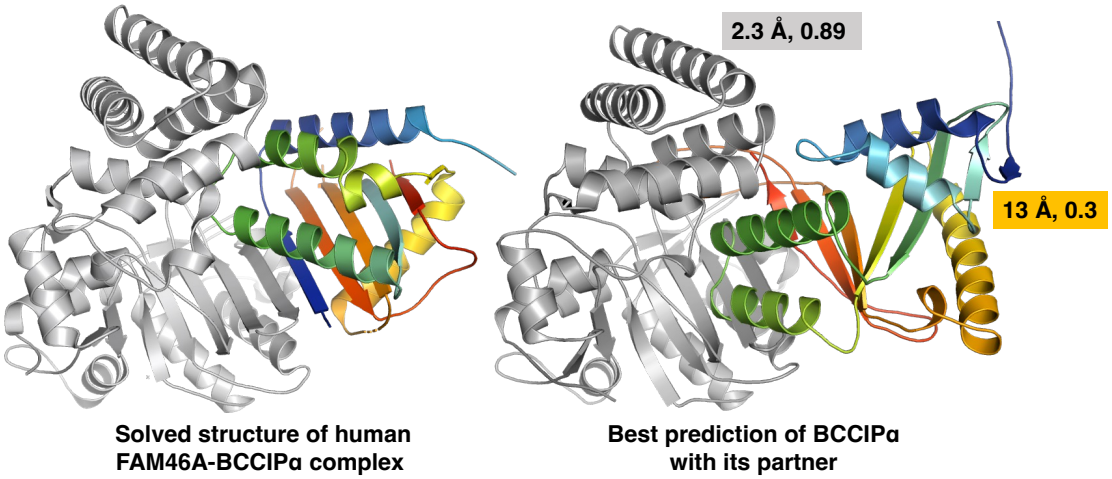

Figure S11. Predicting the structure of BCCIPα with its binding partner using AF2_multimer generated the incorrect BCCIPβ conformation for all models. Structure of the experimentally determined complex (PDB ID: 8EXF, left) differs from all AF2_multimer models (Ranked 1 shown). The structure of BCCIPα's binding partner, FAM46A (gray), was predicted with has high accuracy: TM-score 0.89 and RMSD 2.3 Å. Whereas BCCIPα (rainbow N->C, blue->red) was poorly predicted: TM-score 0.3 and RMSD 13 Å. The predicted binding interface is also incorrect.